Published in final edited form as:
FEBS Lett. 2014 March 18; 588(6): 892–898. doi:10.1016/j.febslet.2014.02.021.

Crystal structure of the RNA demethylase ALKBH5 from zebrafish

Weizhong Chen[a,b,c], **Liang Zhang**[b], **Guanqun Zheng**[b], **Ye Fu**[b], **Quanjiang Ji**[b], **Fange Liu**[b], **Hao Chen**[c], and **Chuan He**[b,*]

[a]Department of Chemical Physics, University of Science and Technology of China, Hefei, Anhui 230026, China

[b]Department of Chemistry and Institute for Biophysical Dynamics, The University of Chicago, 929 E. 57th Street, Chicago, Illinois 60637, USA

[c]Coordination Chemistry Institute and the State Key Laboratory of Coordination Chemistry, School of Chemistry and Chemical Engineering, Nanjing University, Nanjing 210093, China

Abstract

ALKBH5, a member of AlkB family proteins, has been reported as a mammalian N^6-methyladenosine (m^6A) RNA demethylase. Here we report the crystal structure of zebrafish ALKBH5 (fALKBH5) with the resolution of 1.65 Å. Structural superimposition shows that fALKBH5 is comprised of a conserved jelly-roll motif. However, it possesses a loop that interferes potential binding of a duplex nucleic acid substrate, suggesting an important role in substrate selection. In addition, several active site residues are different between the two known m^6A RNA demethylases, ALKBH5 and FTO, which may result in their slightly different pathways of m^6A demethylation.

Keywords

ALKBH5; crystal structure; demethylation; N^6-hydroxymethyladenosine

1. Introduction

Among the various RNA modifications, N^6-methyladenosine (m^6A) is of great interest because it is the most prevalent internal modifications in eukaryotic mRNA [1]. This modification also exists in the virus RNA that is transcribed in host nuclei [2], and plays a important role in yeast meiosis and plant development [3, 4]. A RNA methyltransferase complex with METTL3 as one of the S-adenosylmethionine-binding subunit installs the N^6-position methyl group of m^6A [5]. Our recent discoveries of two m^6A demethylases (FTO and ALKBH5) specifically highlight the importance of the reversal of this modification [6, 7]. Furthermore, the recently mapped transcriptome-wide distributions of m^6A in human and

*Corresponding author. Address: Department of Chemistry and Institute for Biophysical Dynamics, The University of Chicago, 929 E. 57th Street, Chicago, Illinois 60637, USA. chuanhe@uchicago.edu (C. He); Tel: 1-773-702-5061; Fax: 1-773-702-0805.

Appendix A. Supplementary data

Supplementary data associated with this article can be found, in the online version.

mouse cells indicate that this modification could affect a series of biological processes including mRNA splicing, nuclear export, as well as host cellular immune response [8–10].

FTO and ALKBH5 belong to the AlkB family of iron(II)/α-ketoglutarate(α-KG)-dependent dioxygenases [11, 12]. Nine AlkB homologous have been identified in mammals: ALKBH1–8 and FTO, which show different preferences for substrates [13]. AlkB, ALKBH2, and ALKBH3 exhibit demethylation activity of 1-methyladenine (m^1A) and 3-methylcytosine (m^3C) in DNA [14–16]. AlkB and ALKBH3 show higher activity to single-stranded (ss)DNA than double-stranded (ds)DNA, while ALKBH2 prefers dsDNA over ssDNA [16]. ALKBH8 contains a RNA recognition motif, a tRNA methyltransferase domain, and an AlkB-like domain, which could convert 5-carboxy-methyluridine (cm^5U) to (*S*)-5-methoxycarbonyl-hydroxymethyluridine ((*S*)-$mchm^5U$) [17, 18]. FTO, a protein associated with human obesity [19–21], was originally shown to demethylate 3-methylthymine (m^3T) in ssDNA and 3-methyluracil (m^3U) in ssRNA [11, 22]. Recently, our group discovered FTO as the first RNA demethylase that mediates demethylation of m^6A to adenosine (A) [6]. Further research in our group indicates that FTO generated two intermediates (N^6-hydroxymethyladenosine (hm^6A) and N^6-formyladenosine (fm^6A)) during the demethylation process [23], which adds potential complexity to this demethylation regulation [24].

ALKBH5 is the second known m^6A RNA demethylase *in vitro* and *in vivo* [7]. The over-expression of ALKBH5 leads to reduction of the cellular m^6A level, while knockdown of ALKBH5 increases the ratio of m^6A to A in mRNA in human cells and mouse testis [7]. Furthermore, aberrant spermatogenesis and apoptosis were observed in mouse testis when *Alkbh5* gene was knocked-out [7]. Although ALKBH5 and FTO exhibit similar substrate preference, their reaction pathways seem to be different: as we show in this study, ALKBH5 directly converts m^6A to adenosine without any intermediate observed. Whereas, two intermediates of hm^6A and fm^6A were observed in the FTO-mediated m^6A demethylation. Recently, the crystallization conditions for human ALKBH5 (hALKBH5) were published [25]; however, the structure has not been reported. Here we report the crystal structure of a truncated zebrafish ALKBH5 (Protein ID: NP_001070855, residues 38–287, named ΔfALKBH5 here and after), which shares high sequence identity to hALKBH5, as well as the same biological activity. This structure should facilitate our understanding of the substrate-selectivity of the AlkB family proteins, and provide further insights for future investigation into the mechanism of m^6A demethylation.

2. Materials and methods

2.1. Cloning, expression, and purification

The truncated zebrafish ALKBH5 (ΔfALKBH5) gene was PCR-amplified from zebrafish cDNA (Thermo Scientific), and subcloned into PMCSG19 vector by ligation independent cloning (LIC) [26], resulting in the ΔfALKBH5-PMCSG19 plasmid with a His6-tag at N-terminal. The constructed plasmid was transformed in BL21(DE3) strain containing PRK1037 plasmid [26]. Cells grew in LB medium containing 50 ug/mL kanamycin and 100 ug/mL Ampicillin at 37 °C. When OD_{600} reached 0.6, the protein expression was achieved by adding 1 mM isopropyl β-D-1-thiogalactopyranoside (IPTG) under 16 °C for overnight. Cells were harvested and stored at −80 °C for subsequent steps.

The cell pellet was resuspended with 35 mL buffer A (10 mM Tris-HCl, pH 7.4, 500 mM NaCl and 1 mM DTT), and lysed by sonication. After centrifugation, the supernatant was loaded to pre-equilibrated Ni-NTA column and washed with eight column volumes of buffer A. Target protein was eluted with gradient linear buffer B (10 mM Tris-HCl, pH 7.4, 500 mM NaCl, 500 mM imidazole, and 1 mM DTT). After removing the His-tag by overnight

TEV enzyme digestion at 4 °C, the protein solution was applied to MonoS column and eluted with linear concentration of NaCl in 10 mM Tris-HCl, pH 7.4. The eluted fractions were pooled, concentrated, and further purified by gel filtration Superdex200 column in 10 mM Tris-HCl, pH 7.4, 150 mM NaCl, and 1 mM DTT. Over 95% purity of protein was obtained for further use (Supplementary Fig. 1). FTO and hALKBH5 proteins were expressed and purified as reported [7, 22].

2.2. Crystallization and data collection

The sitting-drop vapor diffusion method was employed for the crystallization of ΔfALKBH5/α-KG protein. 1 uL 10 mg/mL protein was mixed with an equal volume of reservoir solution (0.2 M Sodium iodide, pH 7.0, 20% w/v Polyethylene glycol 3,350) in the presence of 1 mM $MnCl_2$ and 2 mM α-KG, and equilibrated against 100 μL of the reservoir solution at 289 K. The crystals of ΔfALKBH5/succinate acid (SIN) were achieved under the same conditions except for the substitution of α-KG for succinate acid. The crystals appeared within 24 hours and were flash-frozen in liquid nitrogen with 25% glycerol (v/v) as the cryoprotectant solution. The crystal diffraction data was collected at the macromolecular crystallography for life science beamline NE-CAT (24-ID-D) at the Advanced Photon Source, Argonne National Laboratory. The data was then integrated and scaled with HKL2000 (Table 1).

2.3. Phasing and Refinement

Zebrafish ALKBH5 structures were resolved by molecular replacement with the CCP4i program PHASER using the structure of *E.coli* AlkB (PDB ID: 2FD8) as the searching model. The structure model building was performed using the computer graphics program Coot, and then refined by using Phenix. The final R/R_{free} factor value of ΔfALKBH5/α-KG and ΔfALKBH5/SIN is 20.9/23.8% and 17.2/18.2%, respectively (Table 1).

2.4. MADLI-TOF/TOF MS analysis

As reported previously [7], 1 nmol 9-mer ssRNA substrate (5'-UAAGm^6ACUCA-3') was mixed with 1 nmol purified ΔfALKBH5/hALKBH5 protein in 100 uL reaction buffer (25 mM HEPES, pH 7.4, 100 mM KCl, 2 mM $MgCl_2$, 0.2 U/μL RNasin, 2 mM L-ascorbic acid, 300 μM α-KG and 150 μM $(NH4)_2Fe(SO4)_2{\cdot}6H_2O$). After incubation at room temperature for 30 min, 10 uL reaction solution was mixed with 50 μl ion exchange resin (Bio-Rad). 1 uL solution was mixed with 1 uL matrix (THAP/Diammonium Citrate) and spotted onto MALDI plate. Then MALDI-TOF/TOF (Bruker) was employed to analyze the results.

2.5. HPLC analysis of ALKBH5 activity

100 uL reaction solution was quenched by 5 mM EDTA followed by heating at 95 °C for 10 min. The reacted ssRNA was digested with 1 uL nuclease P1 at 42 °C for overnight. Then 10 uL 1 M NH_4HCO_3 and 1 uL alkaline phosphatase were added to the solution and digested for 3 h at 37 °C. HPLC system equipped with an Acclaim 120, C18, 5μm analytical column (Dionex, 059148) was employed to analyze the result. 30 uL digested solution was injected in HPLC and eluted with buffer A (50 mM ammonia acetate) and buffer B (60% acetonitrile, 0.01% TFA, 50 mM ammonia acetate) with a flow rate of 1 ml/min. The analysis was executed at room temperature. The detection wavelength was set at 260 nm.

3. Results and discussion

3.1. Sequence identity and biological activity of hALKBH5 and fALKBH5

ALKBH5 shares high sequence identity among different species. Sequence alignment by ClustalW2 indicates that their differences are mainly distributed at the N- and C-termini

with the active site highly conserved, including the five invariant residues (HxD..H..R..R) (Supplementary Fig. 2). After testing ALKBH5 from different species, we succeeded in crystallizing a truncated form of zebrafish ALKBH5 (ΔfALKBH5, residues 38–287) in complex with manganese(II) and α-KG. Full-length fALKBH5 shares 73.9% identity (260/352 residues) with hALKBH5, and the identity for ΔfALKBH5 reaches as high as 80.8% (202/250 residues).

To confirm that the truncation of fALKBH5 did not affect catalytic activity, a 9-mer ssRNA substrate (UAAGm^{6}ACUCA) was treated with equal amounts of hALKBH5 and ΔfALKBH5 for 30 min at room temperature, respectively. MALDI-TOF/TOF was employed to analyze the results. A loss of 14 Da in substrate mass in experiments with both hALKBH5 and ΔfALKBH5 was observed, showing the m^{6}A demethylation activity of ΔfALKBH5 (Fig. 1A). To further confirm this observation, the reacted ssRNA was completely digested using nuclease P1 and alkaline phosphatase to single nucleosides, and then analyzed by HPLC. As shown in Fig. 1B, ΔfALKBH5 could completely demethylate m^{6}A in the ssRNA substrate as hALKBH5.

3.2. The structure of ΔfALKBH5 and its active site

ΔfALKBH5 was crystallized in complex with manganese(II) and α-KG by mixing with an equal volume of reservoir solution (0.2 M sodium iodide, pH 7.0, 20% w/v polyethylene glycol 3,350) at 289 K, and a high-resolution (1.65 Å) x-ray diffraction data set was collected. *E.coli* AlkB, the closest homologue of ALKBH5, shares 14.8% identity (37/250 residues) and 39.2% similarity (98/250 residues) with ΔfALKBH5. Using the structure of AlkB (PDB ID: 2FD8) as a searching model, the final model of ΔfALKBH5 structure was refined to 1.65 Å (Table 1). fALKBH5 is a monomer in solution, and there are two monomers per asymmetric unit in the $P2_12_12_1$ unit cell and they interact with each other mainly through a loop (named L2 here and after) (Supplementary Fig.3). ΔfALKBH5 is composed of 11 β-strands and 3 long α-helixes. As illustrated in Fig. 2, the active site of fALKBH5 is mainly composed of a jelly-roll motif [27], which is formed of eight β-strands (β4-β11). The β sheets are connected through loops and 3 α-helixes buttressing the jelly-roll motif from the outside.

Sequence alignment shows that the consensus HxD..H..R..R residues in the active site of fALKBH5 are highly conserved (Fig. 3A and Supplementary Fig. 2), and structural alignment reveals five invariant residues reside in positions similar to those of other AlkB family proteins (namely, human ALKBH3, hALKBH3; human ALKBH8, hALKBH8; human FTO, FTO; and *E. coli* AlkB, AlkB) (Supplementary Fig. 4). The root-mean-square deviation (rmsd) between fALKBH5 and its homologues is within 3.5 Å (AlkB: 2.46 Å, hALKBH2: 2.62 Å, hALKBH3: 2.61 Å, hALKBH8:1.75 Å, FTO: 3.16 Å). As showed in Fig. 4A and Supplementary Fig. 5, His172, Asp174, and His234 coordinate to manganese(II), and Arg245 interacts with α-KG through a salt bridge. It is noteworthy that the distance between Arg251 (the second arginine in the motif) and α-KG is 4.4 Å, whereas in other AlkB family proteins the corresponding residues are much closer to α-KG with the distance around 3 Å (Fig. 4A and Supplementary Fig. 6) [28–31]. This observation therefore suggests that Arg251 in ΔfALKBH5 may not bind α-KG, which differs from its equivalents in other AlkB homologous. Previous studies have confirmed that the (HxD..H..R..R) motif is highly conserved in all AlkB family members, and the five invariant residues are essential for enzymatic activity [32]. Usually, the second arginine (Arg251 in fALKBH5) is considered as an α-KG-binding residue, but our structure of ΔfALKBH5 shows a potential weaker interaction between Arg251 and α-KG.

α-KG is the cofactor for the oxidation reaction catalyzed by ALKBH5, in which it is converted to succinic acid [13]. The addition of α-KG or succinic acid could help stabilize

fALKBH5 protein and thus facilitates its crystallization. We also obtained the structure of ΔfALKBH5 in complex with manganese(II) and succinic acid at 1.80 Å resolution (Table 1). In both structures, the manganese(II) adopts a hexa-coordination geometry. Besides the three ligand residues (His172, Asp174, and His234) from the protein, two water molecules and succinate occupy the three remaining coordinate sites of the central manganese(II) in this succinate-bound form (Fig. 4B), while one water and two oxygen from α-KG bind the metal in the α-KG-bound form (Fig. 4A).

3.3. Structure and sequence comparison with other AlkB family proteins

An overlap of the current structure with the structure of human ALKBH2(hALKBH2)-dsDNA [33] yielded some interesting observations. We found that the loop L2 in ΔfALKBH5 protruded into the dsDNA strand in the overlapped hALKBH2-dsDNA structure (Fig. 3B). ALKBH5 has been shown to exhibit much higher activity to ssRNA than dsRNA [7]; this L2 loop most likely plays the role of discriminating against duplex nucleic acids. In addition, the basic residues in the loop are prone to form hydrogen bonds with acidic residues, which may act to enhance the binding of fALKBH5 to ssRNA. It is interesting that FTO also has a loop (referred as L1) that clashes with potential duplex nucleic acid substrates [30]. The sequence alignment shows that the L1 loop in FTO is unique among the AlkB family proteins (Fig. 3A). The L2 loop is highly conserved among ALKBH5 in different species, and has no similarity to other AlkB family proteins as well (Fig. 3A and Supplementary Fig. 2). An overlay of the structure of FTO and fALKBH5 revealed further insights. We found that L1 and L2 loops are both close to the active site. However, the two loops extend from the opposite directions (Fig. 3C). The two loops most likely play similar roles in blocking potential dsDNA/RNA from gaining access to the substrate-binding site. In addition, ΔfALKBH5 lacks a lid composed of two β-strands over the active site, which exists in FTO as well as in AlkB, hALKBH2, and hALKBH3 (Fig. 3A and Fig. 3D). Referred as “nucleotide recognition lid” in AlkB, this lid is conformationally flexible and is involved in binding to nucleotide substrates. It has been proposed to play a role in the substrate recognition [31]. hALKBH2, hALKBH3 and FTO also possess similar lids that were assumed to perform the same function [28, 30, 33]. However, this lid is not conserved among other these proteins in the AlkB family (Fig. 3A). Comparing the structures of fALKBH5 and FTO, the lid in FTO covers the active site while its absence in fALKBH5 makes the active site more exposed (Supplementary Fig. 7).

3.4. Residues comparison near active site between FTO and fALKBH5

Among all AlkB family proteins, we are most interested in comparisons between ALKBH5 and another m^6A demethylase, FTO. We first assayed the demethylation of hALKBH5 with m^6A-containing RNA. Under the same conditions that we were able to observe hm^6A and fm^6A intermediates in the FTO-mediated m^6A oxidation, we failed to observe these intermediates in the reaction with hALKBH5 and fALKBH5 (Fig.1A). This observation suggests that ALKBH5 might go through a mechanism of m^6A demethylation slightly different from FTO. Supplementary Fig. 8 illustrates the proposed m^6A demethylation process. FTO could generate intermediates of hm^6A and fm^6A in a step-wise manner when converting m^6A to A, and both hm^6A and fm^6A would decompose to adenosine in aqueous solution with both half-lives of around 3 hrs [23]. By contrast, ALKBH5 demethylates m^6A to A without observing these intermediates. It is possible that ALKBH5 facilitates/catalyzes decomposition of the generated hm^6A when bound to the active site. The exact mechanistic difference related to the production of hm^6A will need further biochemical and computational investigations in the future. As viewed through structural alignment, most of residues are visibly conserved except Lys100, Ile169, and Pro175 between fALKBH5 and FTO, which correspond with Arg96, Val228 and Glu234 in FTO (Fig. 5). These three residues in ALKBH5 are also highly conserved among different species (Supplementary

Fig. 2). As neutral and hydrophobic residues, Ile169 and Val228 may not directly participate in the demethylation process. Glu234 was reported to form a hydrogen bond with m^3T in the FTO-m^3T structure, and the mutation of Glu234 to proline resulted in the loss of FTO activity of demethylating m^3T [30]. As illustrated in Fig. 5, Pro175 lies in the corresponding position in fALKBH5, which could not form the similar hydrogen bond with nucleic substrates. In addition, mutation of Arg96 in FTO to methionine, glutamine or histidine led to loss of FTO demethylation activity [30, 34], while its equivalent residue is Lys100 in fALKBH5. We have mutated Lys100 to arginine and Pro175 to glutamic acid in fALKBH5, respectively, and tested the demethylation activity of both mutant proteins by MALDI-TOF. As showed in Supplementary Fig. 9, a reduced m^6A demethylation activity was observed for ΔfALKBH5 P175E, whereas ΔfALKBH5 K100R almost lost its activity. This result indicated that Lys100 and Pro175 in fALKBH5 are involved in m^6A demethylation. Future mechanistic studies are required to study differences between ALKBH5 and FTO.

4. Conclusions

The non-heme α-KG-dependent AlkB family demethylases mainly catalyze the oxidative demethylation of *N*-alkylated nucleic acid bases. These members posses a similar catalytic core as well as a highly conserved (HxD..H..R..R) motif. Their substrates differ, however. The molecular basis of substrate-selection and reactions mechanisms have attracted much research attention. Here, we present the high resolution structure of fALKBH5 at 1.65 Å. FTO possesses a loop (L1) that is important for ssRNA-binding, while fALKBH5 possesses a different loop (L2) extended from the opposite direction to accomplish the same function. The presence of this loop explains the preference of ALKBH5 for ssRNA. We also show that unlike FTO, which generates hm^6A and fm^6A as intermediates in the process of m^6A demethylation, such intermediates are not observed in demethylation reactions catalyzed by ALKBH5. Differences in active residues between these two proteins, as well as the weaker interaction between Arg251 and α-KG may explain the light difference in the demethylation pathways of these two proteins. In summary, we report the structure of fALKBH5, which provides a molecular basis for the study of substrate-selection specificity in the AlkB family. With this structure now available, future work will focus on elucidating the potential mechanistic differences between FTO and ALKBH5 m^6A demethylation and the potential impact to biology functions.

PDB references

ΔfALKBH5/α-KG 4NPL and ΔfALKBH5/SIN 4NPM.

Supplementary Material

Refer to Web version on PubMed Central for supplementary material.

Acknowledgments

We thank Dr. Kay Perry from NE-CAT for structure data procession and structure determination. S.F. Reichard, MA contributed editing. This work is supported by National Institutes of Health GM071440 (to C.H.). W.C. was partially supported by the China Scholar Program, the National Nature Science Foundation of China (91013009 and 21071077) and the Ministry of Science and Technology of China Key Project (2012CB933802).

Abbreviations

m^6A	N^6-methyladenosine
hm^6A	N^6-hydroxymethyladenosine

fm^{6}A	N^6-formyladenosine
A	adenosine
fALKBH5	zebrafish ALKBH5
α-KG	α-ketoglutarate
m^{1}A	1-methyladenine
m^{3}C	3-methylcytosine
ss	single-stranded
ds	double-stranded
cm^{5}U	5-carboxy-methyluridine
(*S*)-mchm^{5}U	(*S*)-5-methoxycarbonyl-hydroxymethyluridine
m^{3}T	3-methylthymine
m^{3}U	3-methyluracil
ΔfALKBH5	truncated zebrafish ALKBH5
IPTG	isopropyl β-D-1-thiogalactopyranoside
SIN	succinate acid
hALKBH3	human ALKBH3
hALKBH8	human ALKBH8
hALKBH2	human ALKBH2
rmsd	root-mean-squaredeviation deviation

References

1. Bokar JA. The biosynthesis and functional roles of methylated nucleosides in eukaryotic mRNA. Fine-tuning of RNA functions by modification and editing, topics in current genetics. 2005 Springer;12:141–177.
2. Beemon K, Keith J. Localization of N6-methyladenosine in the Rous sarcoma virus genome. J. Mol. Biol. 1977; 113:165–179. [PubMed: 196091]
3. Shah J, Clancy M. IME4, a gene that mediates MAT and nutritional control of meiosis in *Saccharomyces cerevisiae*. Mol. Cell. Biol. 1992; 12:1078–1086. [PubMed: 1545790]
4. Bodi Z, Zhong S, Mehra S, Song J, Graham N, Li H, May S, Fray RG. Adenosine methylation in *Arabidopsis* mRNA is associated with the 3′ end and reduced levels cause developmental defects. Front. Plant Sci. 2012; 48:1–9.
5. Bokar J, Shambaugh M, Polayes D, Matera A, Rottman F. Purification and cDNA cloning of the AdoMet-binding subunit of the human mRNA (N6-adenosine)-methyltransferase. RNA. 1997; 3:1233–1247. [PubMed: 9409616]
6. Jia G, Fu Y, Zhao X, Dai Q, Zheng G, Yang Y, Yi C, Lindahl T, Pan T, Yang YG, He C. N6-methyladenosine in nuclear RNA is a major substrate of the obesity-associated FTO. Nat. Chem. Biol. 2011; 7:885–887. [PubMed: 22002720]
7. Zheng G, Dahl JA, Niu Y, Fedorcsak P, Huang CM, Li CJ, Vågbø CB, Shi Y, Wang WL, Song SH, Lu Z, Bosmans RPG, Dai Q, Hao YJ, Yang X, Zhao WM, Tong WM, Wang XJ, Bogdan F, Furu K, Fu Y, Jia G, Zhao X, Liu J, Krokan HE, Klungland A, Yang YG, He C. ALKBH5 is a mammalian RNA demethylase that impacts RNA metabolism and mouse fertility. Mol. Cell. 2012; 49:18–29. [PubMed: 23177736]

8. Dominissini D, Moshitch-Moshkovitz S, Schwartz S, Salmon-Divon M, Ungar L, Osenberg S, Cesarkas K, Jacob-Hirsch J, Amariglio N, Kupiec M, Sorek R, Rechavi G. Topology of the human and mouse m6A RNA methylomes revealed by m6A-seq. Nature. 2012; 485:201–206. [PubMed: 22575960]
9. Meyer KD, Saletore Y, Zumbo P, Elemento O, Mason CE, Jaffrey SR. Comprehensive analysis of mRNA methylation reveals enrichment in 3' UTRs and near stop codons. Cell. 2012; 149:1635–1646. [PubMed: 22608085]
10. Karikó K, Buckstein M, Ni H, Weissman D. Suppression of RNA recognition by Toll-like receptors: the impact of nucleoside modification and the evolutionary origin of RNA. Immunity. 2005; 23:165–175. [PubMed: 16111635]
11. Gerken T, Girard CA, Tung YCL, Webby CJ, Saudek V, Hewitson KS, Yeo GS, McDonough MA, Cunliffe S, McNeill LA, Galvanovskis J, Rorsman P, Robins P, Prieur X, Coll AP, Ma M, Jovanovic Z, Farooqi IS, Sedgwick B, Barroso I, Lindahl T, Ponting CP, Ashcroft FM, O'Rahilly S, Schofield CJ. The obesity-associated FTO gene encodes a 2-oxoglutarate-dependent nucleic acid demethylase. Science. 2007; 318:1469–1472. [PubMed: 17991826]
12. Kurowski MA, Bhagwat AS, Papaj G, Bujnicki JM. Phylogenomic identification of five new human homologs of the DNA repair enzyme AlkB. BMC Genomics. 2003; 4:48. [PubMed: 14667252]
13. Yi C, Yang CG, He C. A non-heme iron-mediated chemical demethylation in DNA and RNA. Acc. Chem. Res. 2009; 42:519–529. [PubMed: 19852088]
14. Trewick SC, Henshaw TF, Hausinger RP, Lindahl T, Sedgwick B. Oxidative demethylation by Escherichia coli AlkB directly reverts DNA base damage. Nature. 2002; 419:174–178. [PubMed: 12226667]
15. Falnes PØ, Johansen RF, Seeberg E. AlkB-mediated oxidative demethylation reverses DNA damage in *Escherichia coli*. Nature. 2002; 419:178–182. [PubMed: 12226668]
16. Aas PA, Otterlei M, Falnes PØ, Vågbø CB, Skorpen F, Akbari M, Sundheim O, Bjørås M, Slupphaug G, Seeberg E, E Krokan H. Human and bacterial oxidative demethylases repair alkylation damage in both RNA and DNA. Nature. 2003; 421:859–863. [PubMed: 12594517]
17. Fu Y, Dai Q, Zhang W, Ren J, Pan T, He C. The AlkB Domain of Mammalian ABH8 Catalyzes Hydroxylation of 5-Methoxycarbonylmethyluridine at the Wobble Position of tRNA. Angew. Chem. Int. Ed. 2010; 49:8885–8888.
18. van den Born E, Vågbø CB, Songe-Møller L, Leihne V, Lien GF, Leszczynska G, Malkiewicz A, Krokan HE, Kirpekar F, Klungland A, Falnes PØ. ALKBH8-mediated formation of a novel diastereomeric pair of wobble nucleosides in mammalian tRNA. Nat. Commun. 2011; 2:172. [PubMed: 21285950]
19. Dina C, Meyre D, Gallina S, Durand E, Körner A, Jacobson P, Carlsson LM, Kiess W, Vatin V, Lecoeur C, Delplanque J, Vaillant E, Pattou F, Ruiz J, Weill J, Levy-Marchal C, Horber F, Potoczna N, Hercberg S, Stunff CL, Bougnères P, Kovacs P, Marre M, Balkau B, Cauchi Sp, Chèvre JC, Froguel P. Variation in FTO contributes to childhood obesity and severe adult obesity. Nat. Genet. 2007; 39:724–726. [PubMed: 17496892]
20. Frayling TM, Timpson NJ, Weedon MN, Zeggini E, Freathy RM, Lindgren CM, Perry JR, Elliott KS, Lango H, Rayner NW, shield B, Harries LW, Barrett JC, Ellard S, Groves CJ, Knight B, Patch AM, Ness AR, Ebrahim S, Lawlor DA, Ring SM, Ben-Shlomo Y, Jarvelin MR, Sovio U, Bennett AJ, Melzer D, Ferrucci L, Loos RJF, Barroso I, Wareham NJ, Karpe F, Owen KR, Cardon LR, Walker M, Hitman GA, Palmer CNA, Doney ASF, Morris AD, Smith GD, Hattersley AT, McCarthy MI. A common variant in the FTO gene is associated with body mass index and predisposes to childhood and adult obesity. Science. 2007; 316:889–894. [PubMed: 17434869]
21. Scuteri A, Sanna S, Chen WM, Uda M, Albai G, Strait J, Najjar S, Nagaraja R, Orrú M, Usala G, Dei M, Lai S, Maschio A, Busonero F, Mulas A, Ehret GB, Fink AA, Weder AB, Cooper RS, Galan P, Chakravarti A, Schlessinger D, Cao A, Lakatta E, Abecasis GR. Genome-wide association scan shows genetic variants in the FTO gene are associated with obesity-related traits. PLoS Genet. 2007; 3:e115. [PubMed: 17658951]
22. Jia G, Yang CG, Yang S, Jian X, Yi C, Zhou Z, He C. Oxidative demethylation of 3-methylthymine and 3-methyluracil in single-stranded DNA and RNA by mouse and human FTO. FEBS Lett. 2008; 582:3313–3319. [PubMed: 18775698]

23. Fu Y, Jia G, Pang X, Wang RN, Wang X, Li CJ, Smemo S, Dai Q, Bailey KA, Nobrega MA, Han KL, Cui Q, He C. FTO-mediated formation of N6-hydroxymethyladenosine and N6-formyladenosine in mammalian RNA. Nat. Commun. 2013; 4:1798. [PubMed: 23653210]
24. He C. Grand challenge commentary: RNA epigenetics? Nat. Chem. Biol. 2010; 6:863–865. [PubMed: 21079590]
25. Zhou B, Han Z. Crystallization and preliminary X-ray diffraction of the RNA demethylase ALKBH5. Acta Crystallogr. F. 2013; 69:1231–1234.
26. Donnelly MI, Zhou M, Millard CS, Clancy S, Stols L, Eschenfeldt WH, Collart FR, Joachimiak A. An expression vector tailored for large-scale, high-throughput purification of recombinant proteins. Protein Expres. Purif. 2006; 47:446–454.
27. Costas M, Mehn MP, Jensen MP, Que L. Dioxygen activation at mononuclear nonheme iron active sites: enzymes, models, and intermediates. Chem. Rev. 2004; 104:939–986. [PubMed: 14871146]
28. Sundheim O, Vågbø CB, Bjørås M, Sousa MM, Talstad V, Aas PA, Drabløs F, Krokan HE, Tainer JA, Slupphaug G. Human ABH3 structure and key residues for oxidative demethylation to reverse DNA/RNA damage. EMBO J. 2006; 25:3389–3397. [PubMed: 16858410]
29. Pastore C, Topalidou I, Forouhar F, Yan AC, Levy M, Hunt JF. Crystal structure and RNA binding properties of the RNA recognition motif (RRM) and AlkB domains in human AlkB homolog 8 (ABH8), an enzyme catalyzing tRNA hypermodification. J. Biol. Chem. 2012; 287:2130–2143. [PubMed: 22065580]
30. Han Z, Niu T, Chang J, Lei X, Zhao M, Wang Q, Cheng W, Wang J, Feng Y, Chai J. Crystal structure of the FTO protein reveals basis for its substrate specificity. Nature. 2010; 464:1205–1209. [PubMed: 20376003]
31. Yu B, Edstrom WC, Benach J, Hamuro Y, Weber PC, Gibney BR, Hunt JF. Crystal structures of catalytic complexes of the oxidative DNA/RNA repair enzyme AlkB. Nature. 2006; 439:879–884. [PubMed: 16482161]
32. Mishina Y, Duguid EM, He C. Direct reversal of DNA alkylation damage. Chem. Rev. 2006; 106:215–232. [PubMed: 16464003]
33. Yang CG, Yi C, Duguid EM, Sullivan CT, Jian X, Rice PA, He C. Crystal structures of DNA/RNA repair enzymes AlkB and ABH2 bound to dsDNA. Nature. 2008; 452:961–965. [PubMed: 18432238]
34. Meyre D, Proulx K, Kawagoe-Takaki H, Vatin V, Gutiérrez-Aguilar R, Lyon D, Ma M, Choquet H, Horber F, Van Hul W, Van Gaal L, Balkau B, Visvikis-Siest S, Pattou Fo, Farooqi IS, Saudek V, O'Rahilly S, Froguel P, Sedgwick B, Yeo GS. Prevalence of loss-of-function FTO mutations in lean and obese individuals. Diabetes. 2010; 59:311–318. [PubMed: 19833892]

Highlights

- The crystal structure of ALKBH5 from zebrafish.
- fALKBH5 is comprised of a conserved jelly-roll motif.
- fALKBH5 possesses a loop discriminating against duplex nucleic acids.
- Several active site residues are different between fALKBH5 and FTO.
- The structure may help understand the RNA demethylation mechanism.

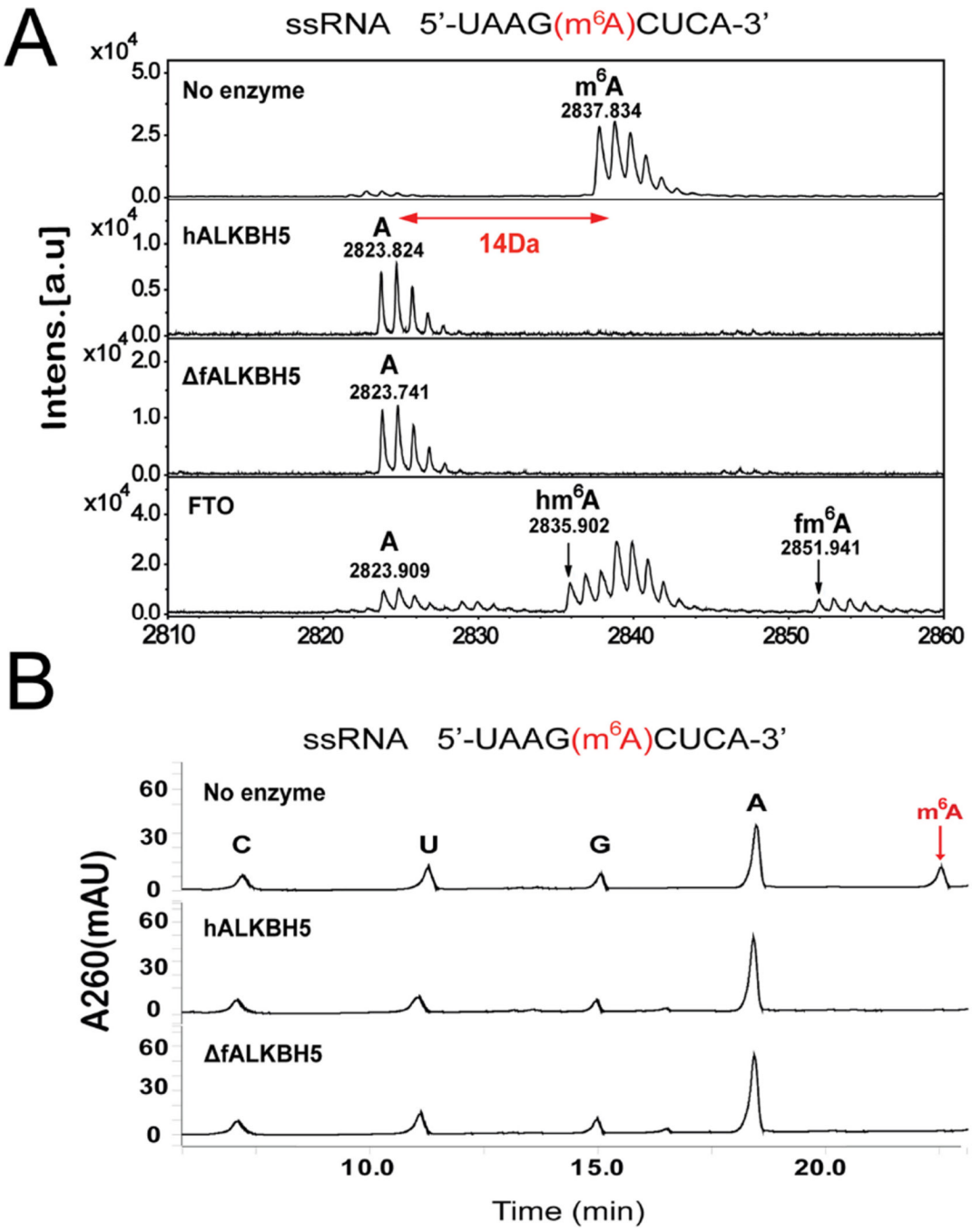

Fig. 1.

(A) MALDI-TOF/TOF mass spectrometry analysis. hALKBH5 and ΔfALKBH5 showed the same activity of m^6A demethylation on ssRNA (ssRNA 5'-UAAGm^6ACUCA-3') with loss of 14-Dalton of a methyl group after the reaction in both cases. By contrast, after treating FTO with ssRNA, two intermediates hm^6A (m^6A-2Da, lost a H_2O moiety during MALDI-TOF ionization) and fm^6A (m^6A+14Da) were observed. The two intermediates were not observed in the reaction with hALKBH5 and ΔfALKBH5 under the same condition. **(B)** HPLC chromatograms of digested nucleosides from m^6A-containing ssRNA. HPLC

confirmed the observation that after treatment with hALKBH5 and ΔfALKBH5, m^6A underwent complete conversion to adenosine.

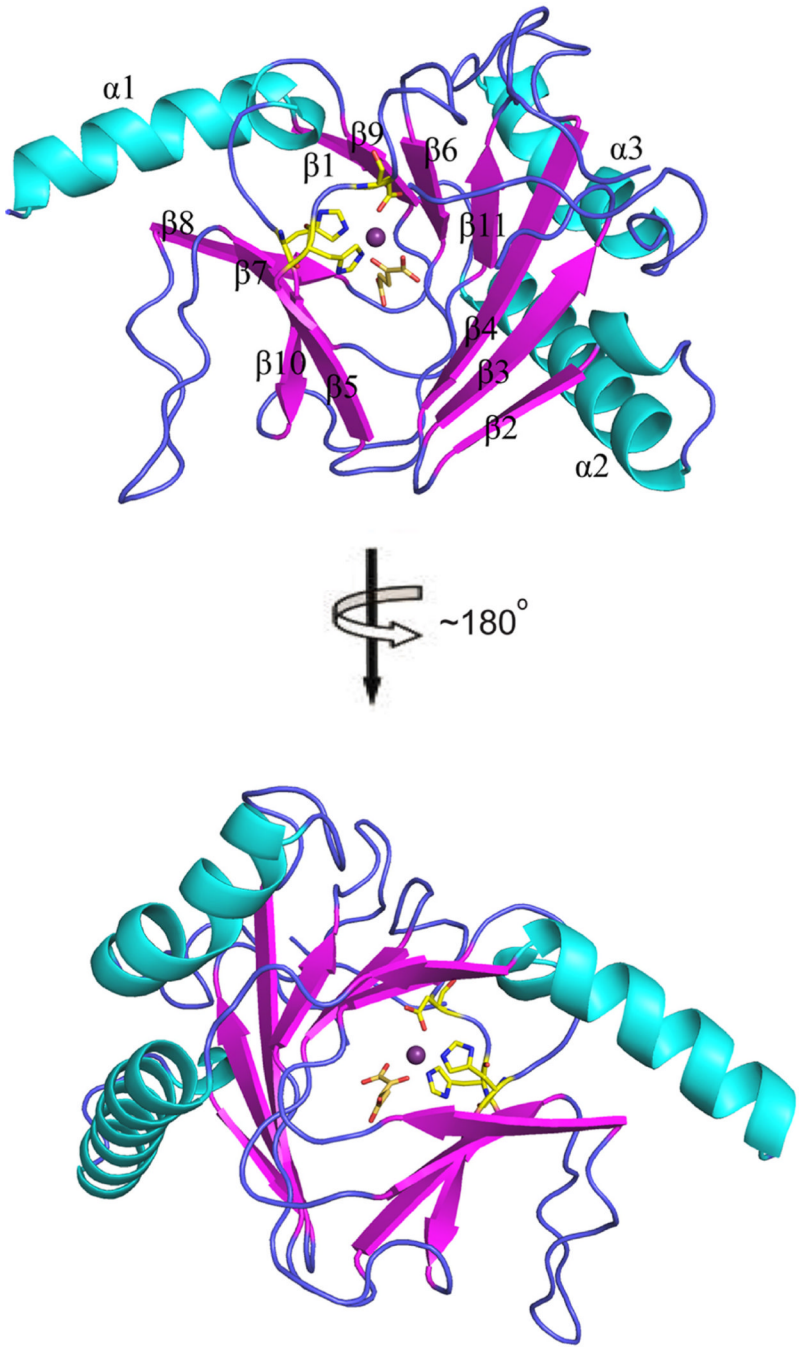

Fig. 2.

The crystal structure of ΔfALKBH5. Two orthogonal views with catalytic core shown. The secondary structural elements are labeled α1-α3 for helices (colored cyan) and β1-β11 for strands (colored magenta).

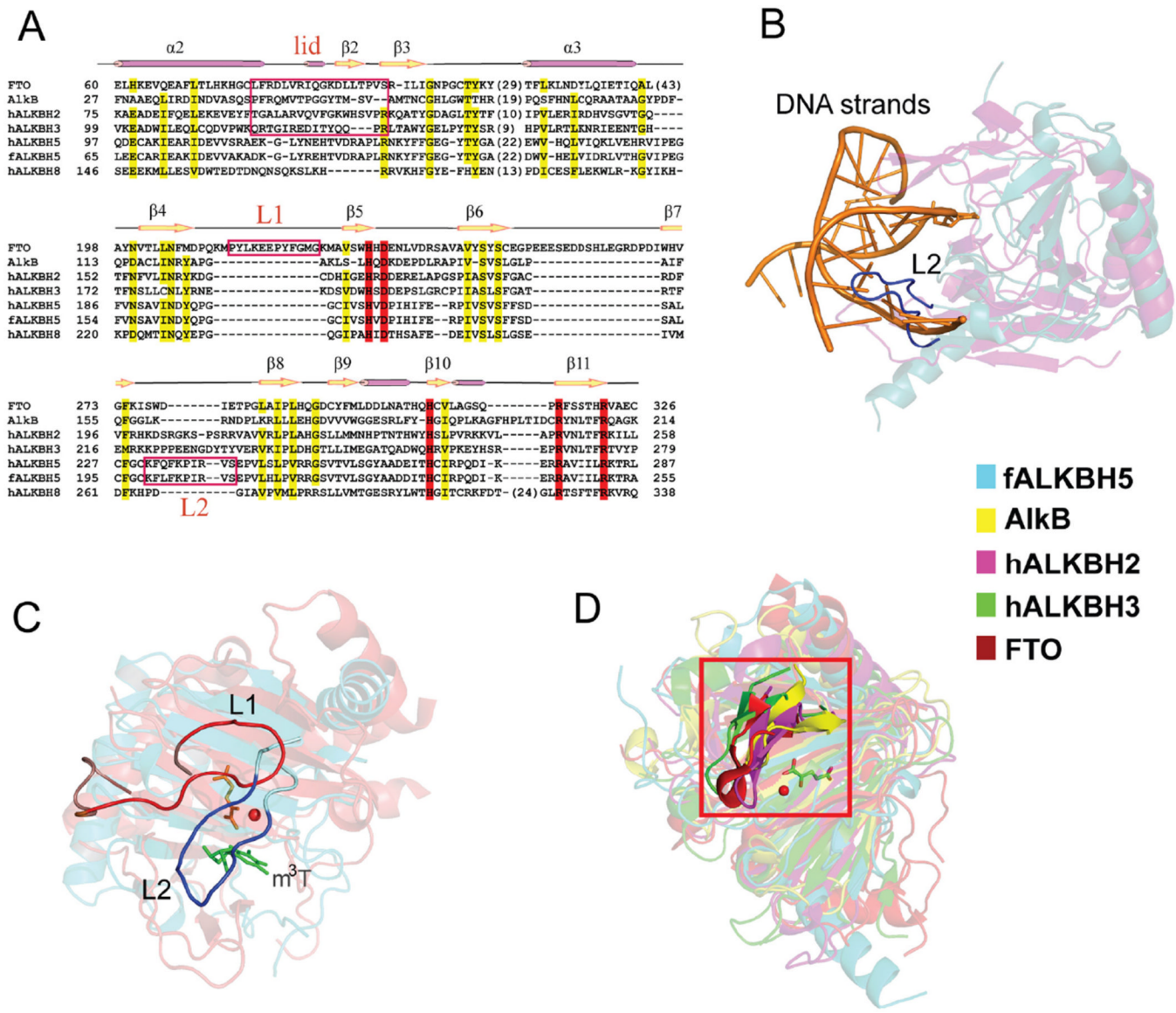

Fig. 3.

The sequence and structure alignment of AlkB family members (FTO (PDB ID: 3LFM), hALKBH2 (PDB ID: 3BTX), hALKBH3 (PDB ID: 2IUW), AlkB (PDB ID: 2FD8), hALKBH8 and fALKBH5). **(A)** Structure-based sequence alignment of AlkB family proteins. The five invariant residues are highlighted in red. The loop L1 in FTO, L2 in human and fish ALKBH5 as well as the lid in FTO, hALKBH2, hALKBH3 and AlkB are boxed off in red. The secondary structure of fALKBH5 is shown on top of the alignment. **(B)** Structural comparison of fALKBH5 and hALKBH2-DNA. The L2 loop (colored in blue) in fALKBH5 protrudes into the dsDNA strand (colored in orange) from the superimposed hALKBH2-dsDNA structure. **(C)** Structure alignment of fALKBH5 and FTO with the extra loop highlighted. (L1 in FTO is colored red, and L2 in fALKBH5 is colored blue.) **(D)** A hairpin creates a lid over the active site in FTO, AlkB, hALKBH2 and hALKBH3. The structure of fALKBH5 lacks such a lid. The lid is highlighted in a red box.

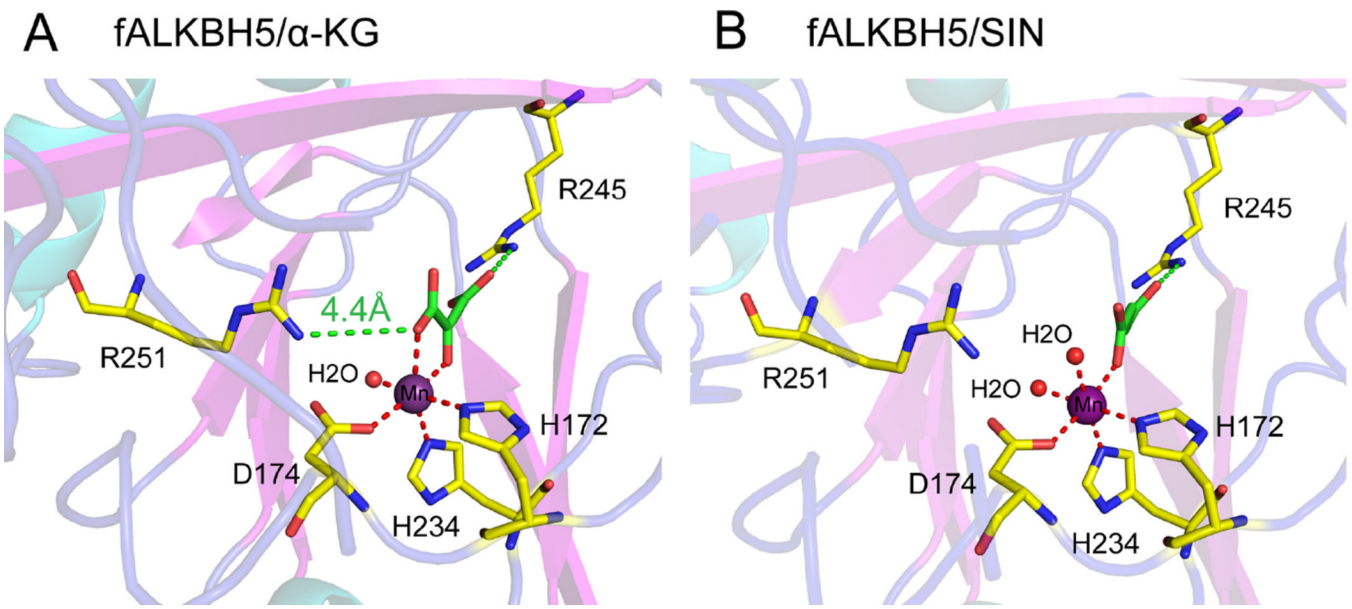

Fig. 4.

The interaction network around Mn(II) and α-KG **(A)** or succinate **(B)**. The coordinate bonds between Mn(II) and its ligands are shown with red dash lines, whereas the interactions between Arg245/Arg251 and α-KG/SIN are indicated in green. The distance between Arg251 and α-KG is 4.4 Å, indicating a weak interaction between them.

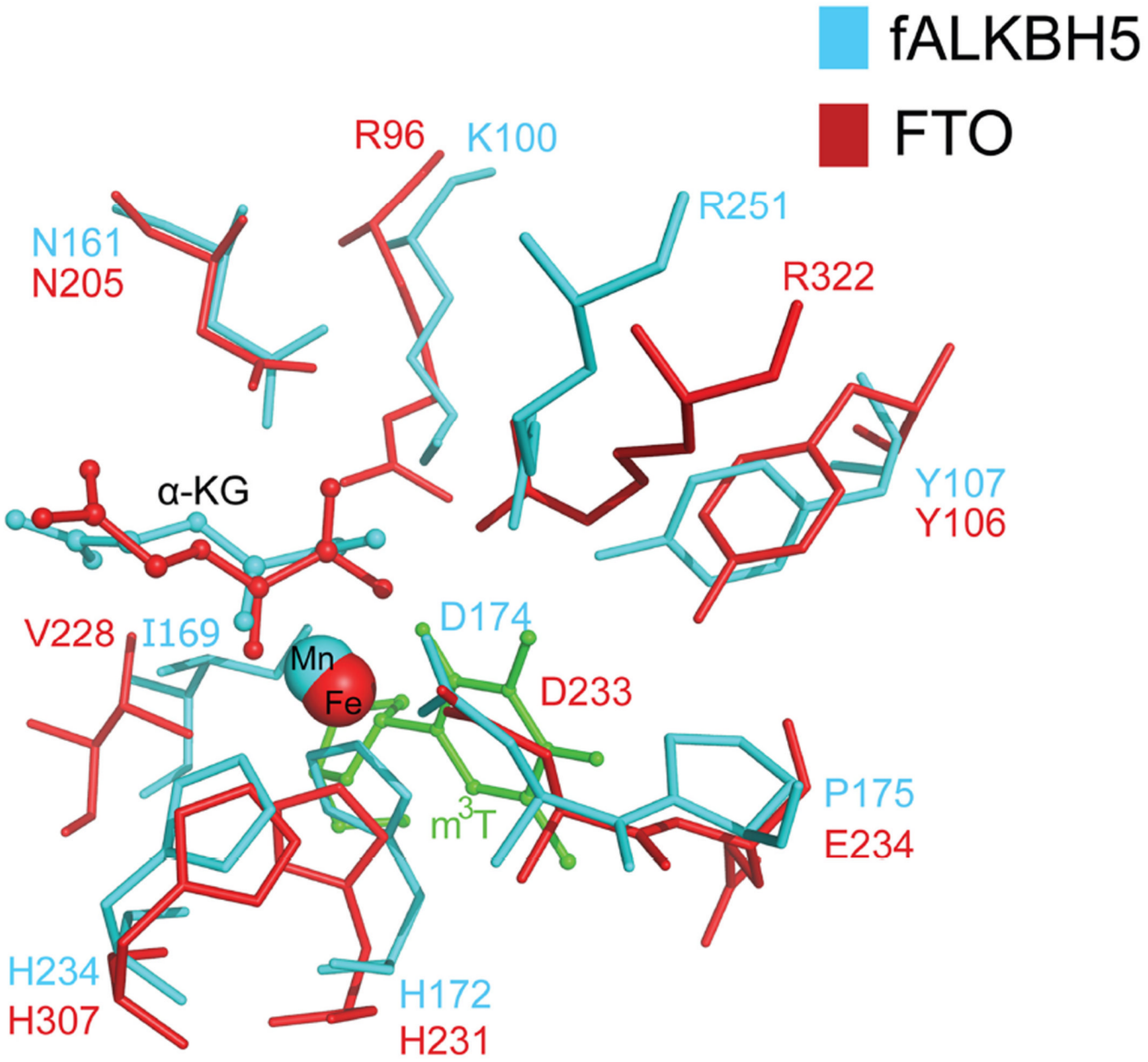

Fig. 5.

Superimposition of residues near the catalytic core in fALKBH5 and FTO. The mononucleotide m^3T in FTO is colored green and residues in fALKBH5 and FTO are labeled in cyan and red, respectively.

Table 1

Data collection and refinement statistics of ΔfALKBH5 in complex with α-KG or succinate acid (SIN).

	ΔfALKBH5/α-KG	ΔfALKBH5/SIN
Data collection		
Space group	$P2_12_12_1$	$P2_12_12_1$
Cell dimensions		
a, *b*, *c* (Å)	65.948, 68.595, 114.909	66.067, 69.792, 115.050
α, β, γ (°)	90.00, 90.00, 90.00	90.00, 90.00, 90.00
Resolution (Å)	30–1.65	50–1.80
R_{sym} or R_{merge}	8.9 (49.0)*	6.9 (59.4)
I / σI	27.8 (3.0)	22.5 (3.5)
Completeness (%)	96.1 (93.2)	99.9 (99.9)
Redundancy	5.7 (4.8)	6.4 (6.5)
Refinement		
Resolution (Å)	30–1.65 (1.71–1.65)	50–1.80 (1.86–1.80)
No. unique reflections	60,317	49,614
R_{work} / R_{free}	20.9/23.8	17.2/18.2
No. atoms		
Protein	3,406	3,370
Ligand/ion	22	18
Water	445	471
B-factors		
Protein	19.8	25.3
Ligand/ion	29.9	29.0
Water	30.1	37.2
R.m.s. deviations		
Bond lengths (Å)	0.007	0.009
Bond angles (°)	1.140	1.161

* Highest-resolution shell is shown in parentheses.